140 KSME Journal, Vol.5, No.2, pp. 140~148, 1991

AN ESTIMATION OF BALLISTIC LIMIT FOR CERAMIC-FRP COMPOSITE ARMOR

Ki Ju Kang* and Kyu Zong Cho*

(Received Jure 1, 1991)

An analytic method is proposed to estimate ballistic limits of ceramic-FRP composite armors. In this method the ballistic limit is evaluated using energy balance approach, that is, the kinetic energy of a projectile just before striking against the armor is assumed to be equal to the sum of energies absorbed during the penetration. The absorbed energies are divided into three parts as follows ; the ones absorbed during the penetration into the ceramic facing and the FRP backing, respectively, and the elastic deformation energy of FRP backing. Through comparisons with Wilkins' experimental results this method is shown to be effective to estimate the ballistic limit of composite armors which consist of 4.064mm to 8.635mm thick AD85 ceramic plate and 4.445mm to 9.525mm thick glass FRP plate.

Key Words : Ceramic-FRP Composite Armor, Ballistic Performance, Penetration, Energy Balance, Elastic Deformation of FRP Plate

NOMENCLATURE

D : Diameter of projectile
D_p : Stiffness of plate
E : Young's modulus
E_0 : Kinetic energy just before strike
E_1 : Energy absorbed during penetration of ceramic facing
E_2 : Energy absorbed during elastic deformation of FRP backing
E_3 : Energy absorbed during penetration of FRP backing
ε_f : Fracture strain
M : Mass of projectile
ρ : Distance from apex of ceramic fracture conoid
p : Pressure transmitted from ceramic to FRP backing
r : Radius
r_p : Radius of elastically deformed area in FRP backing
ϕ : A half apex angle of ceramic fracture conoid
T_c : Thickness of ceramic facing
T_f : Thickness of FRP backing
V_{bl} : Ballistic limit velocity
w : Displacement in z-direction
σ_t : Tensile strength
σ_c : Compressive yield stress
σ_s : Effective strength of ceramic

1. INTRODUCTION

Since ceramic-FRP composite plates were found to be very effective armors in early 1960's, numerous works have been carried out to investigate the protection mechanism and to improve the performance. Many experiments have been performed to evaluate the ballistic limits of the effective materials and their combination (Stiglich, 1968 ; Kim and Palmour, 1970 ; Torti and Herrick, 1971 ; Landingham and Casey, 1972 ; Cardner, 1975 ; Gulbierz and Bohan, 1980). And many other studies have been concentrated to analyze the protection mechanism (Wilkins, 1968 ; Martin, 1969 ; Cline and Wilkins, 1969 ; Bodine et al., 1969 ; Florence, 1969 ; Wilkins et al., 1969 ; Wilkins et al., 1971). As the results of experiments and computational works, the penetration procedure through ceramic composite armors is explained as follows (see Fig.1). As soon as a projectile strikes the ceramic plate, due to high compressive strength of the ceramic, the tip of the projectile being shattered or blunted, which would increasing the projectile-ceramic contact area and relaxing the stress concentration consequently. In a while, the compressive shock waves would propagate into the ceramic and the backing material. During the propagation of the shock waves, a conically fractured ceramic body whose apex is located near the impact point will be developed with accompanying the many radial and circumferental cracks. After passing through the ceramic body, the compressive waves would also deform the backing material. The elastic and plastic deformation zone of the backing material would nearly equal to the base area of the conoidal fracture volume. Finally all the penetration procedures are finished where after the residual projectile or fragments, which coming through the ceramic, strike on the deformed backing plate.

However, depite of considerable results of the previous researches, unlike a simple metal armors, the influences of dimension and property of ceramic facing and backing plate on the ballistic performance have not been fully clarified. So any reliable design procedure has not been established yet, that the cost consuming experiments have been required still now.

Here we propose an analytic method to estimate the ballistic limit velocity of ceramic composite armors. In this method, the kinetic energy loss of a projectile between before and after the penetration are assumed to be equal to the sum of energies which are absorbed during the each stage of the penetration procedures. The each energy term is evaluated

*Department of Machine Design Engineering, Chonnam National University, 300 Yongbongdong Kwangju 500-757, Korea

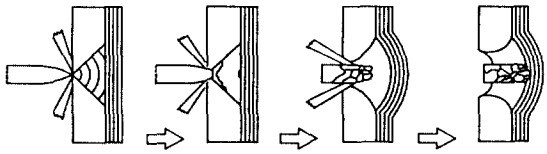

Fig. 1 Illustrations of penetration procedure in ceramic/FRP composite armour.

quantitatively through a simple calculation.

2. THEORY

2.1 The Energy Balance

In order to estimate the ballistic limit velocity of a ceramic-FRP composite armor, an analytic model is constructed as illustrated in Fig.2. The kinetic energy losses between before and after the penetration are assumed to be equal to the sum of energies which are absorbed during penetration as follows ;

$$E_0 - E_r = E_1 + E_2 + E_3 \tag{1}$$

where E_0 and E_r are the kinetic energy of projectile before and after penetration respectively. The right hand terms of E_1, E_2, E_3 are absorbed energies during penetration into the ceramic facing (see Fig.2(a)), during deformation of the FRP backing (see Fig.2(b)) and during penetration into the FRP backing (see Fig.2(c)) respectively.

E_0 and E_r are represented by

$$E_0 = \frac{1}{2} M V_s^2$$

$$E_r = \frac{1}{2} M_r V_r^2$$

where M and M_r are initial and residual mass of the projectile respectively, and V_s and V_r are initial striking velocity and residual velocity respectively.

2.2 Penetration of Ceramic Facing

The absorbed energy, E_1, during penetration of the ceramic facing, consists of the fracture energy of the ceramic, the deformation and fracture energy of the projectile, and the energies converted into heat, light, sound and so on. But it is impossible to calculate the each term theoretically.

Rosenberg et al. proposed a new parameter as 'ballistic efficiency' to describe the ballistic performance of ceramics (Rozenberg and Yeshurun, 1987 ; Bless, Rozenberg and Yoon, 1987 ; Rozenberg and Yeshurun, 1988). In the progress

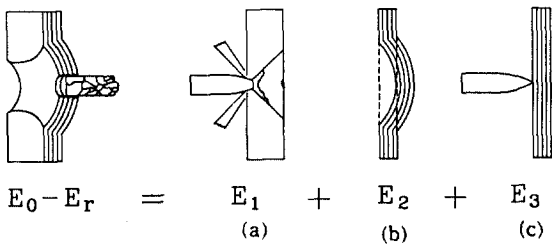

Fig. 2 A penetration model to evaluate ballistic limit.

to prove validity of the parameter, they cited the equation which Forrestal et al.(1987) had presented for metal armors, and slightly modified the equation as (Rozenberg, 1988)

$$\frac{1}{2} M V_{bl}^2 = \frac{\pi D^2}{4} T \sigma_p \tag{2}$$

where V_{bl} is ballistic limit, D is diameter of a projectile, T is thickness of a ceramic plate, and σ_p is a compressive strength of the ceramic. Since $\pi D^2/4$ is cross-sectional area of the projectile, the Eq. (2) means that the ceramic is perforated due to compressive yielding in a small volume whose cross-sectional area is equal to the one of the projectile. The equation agrees with the classical Robin-Euler theory for simple metal armors.

The target which Rosenberg et al.(1987, 1988) were used to measure the ballistic efficiency was consisted of a ceramic facing and a very thick aluminum block, that is, a high stiff backing. This configuration enables the ceramic to act at the highest compressive strength for defeating the projectiles. Therefore, it is reasonable that they applied Eq.(2) to verify a relation between the ballistic efficiency and the compressive strength of ceramics. But in the generally used ceramic-FRP composite armors, the stiffness of backing is relatively low, so that the tensile failure being developed first at the back surface of ceramics. consequently, the effective strength will be used instead of the compressive strength during the absorbed energy calculation for the penetration phenomena. The effective strength is defined as follow ;

$$\sigma_s = \sigma_{cc} \tan h\left[\frac{D_{pc}\varepsilon_{fc} + D_{pf}\varepsilon_{ff}}{B}\right] \tag{3}$$

where σ_{cc} is the compressive strength of the ceramic, B is a constant and ε_{fc}, ε_{ff} are the fracture strain of the ceramic and FRP, respectively. Also, D_{pc} and D_{pf} are the stiffness of the ceramic facing and FRP backing respectively, which were given by (Szilard, 1974)

$$D_p = \frac{ET^3}{12(1-\nu^2)}$$

Since the ceramic and FRP show little plastic deformation during their fracture, the constitutive relationship between the fracture strain ε_f and the fracture stress σ_f, would be linearly assumed

$$\sigma_f = E\varepsilon_f.$$

Here the fracture stress σ_f's are nearly equal to tensile strength σ_t's. Consequently, Eq.(3) can be replaced by

$$\sigma_s = \sigma_{cc} \tan h\left[\frac{1}{B}\left[\frac{\sigma_{tc} T_c^3}{12(1-\nu_c^2)} + \frac{\sigma_{tf} T_f^3}{12(1-\nu_f^2)}\right]\right] \tag{4}$$

Also, taking into account of the conoidal shape of the fracture ceramic volume, the absorbed energy E_1 can be expressed as,

E_1 = (volume of fractured ceramic) × (effective strength of ceramic)

$$= \pi T_c\left[\frac{D^2}{4} + \frac{DT_c}{2}\tan\phi + \frac{T_c^2}{3}\tan^2\phi\right]\sigma_s. \tag{5}$$

where ϕ is a half apex angle of the conoid and σ_s is given by Eq.(4).

2.3 Deformation of the FRP Backing Plate

As shown in Fig.1, the FRP backing is deformed under the compressive forces transmitted from the ceramic facing. The FRP consists of fibrous elements and plastic compound matrix whose strength is relatively poor. The fibrous elements show elastic stress-strain behavior nearly until their failure. In case of woven Roving FRP, the interfacial lamina shear failurer is less occurred then the layered matrix FRP. Therefore, It can be assume that the FRP backing being deformed linear elastically until its failure. Since the deformation occurs only in a area nearly equal to the bottom of ceramic fracture conoid, as mentioned above, the deformation energy E_2 can be evaluated through linear elastic analysis of an axi-symmetrically loaded circular plate with clamped boundaries.

FDM analyses mof Evans et al.(1976) showed that when a rigid sphere struck on a plane, the contact pressure decreased from its maximum and approached gradually to a constant value. On the other while, the maximum pressure was proportional to striking velocity (V_s). Wilkins (1968), however, reported that just after a AP projectile struck on a ceramic composite armor, not only its sharp tip being broken down but also the maximum pressure arising time being somewhat delayed. We assume that, in spite of the time delay, maximum pressure σ_{max} is still proportional to the striking velocity as

$$\sigma_{max}=kV_s \tag{6}$$

where k is a material constant.

Here, it can be supposed that the maximum contact pressure will generate the shock wave, and then which the maximum pressure wave front being transmitted to the backing material. Therefore the maximum deformation will be occur on the backing material during the first wave front being passed the backing material. In order to analyze the backing material deformation, the force balance equation has to be set up in Z direction. Refer to the Fig.3, between the maximum contact pressure σ_{max} and transmitted normal stress $\sigma_{\rho\rho}$, the balancing equation will be

$$\sigma_{max}\frac{\pi D^2}{4}=\int_0^{\phi}\sigma_{\rho\rho}2\pi\rho\sin\theta\cos\theta\rho d\theta \tag{7a}$$

where, ρ is a distance from O, and θ is an angle from z-axis. Where $\sigma_{\rho\rho}$ is independent on θ. Eq.(7a) can be replaced with

$$\sigma_{\rho\rho}=\sigma_{max}\left[\frac{D}{2\rho\ \sin\theta}\right]^2 \tag{7b}$$

As the compressive wave front being to reach the interface, the backing material being to deform (due to the pressure accompanied by the wave). With ignoring any friction or adhesion effect at the interface, it can be assume that the pressure 'p' transmitted to the backing is equal to the z-directional component of $\sigma_{\rho\rho}$ in Eq. (7b). Consequently, 'p' is expressed as

$$p=\sigma_{\rho\rho}\cos\theta=\sigma_{max}\left[\frac{D}{2\rho\ \sin\theta}\right]^2\cos\theta. \tag{8}$$

Substituting Eq. (6) and a geometrical relation between ρ and r in to Eq. (8), 'p' can be represented as follow;

$$p=C\frac{V_s}{[(T_c+\frac{D}{2}\cot\phi)^2+r^2]}\cos\theta \tag{9a}$$

were

$$C=\frac{k}{\pi\sin^2\phi},$$

that is, C is not dependent on the impact velocity but a material constant. on the other hand, the θ is given by

$$\theta=\tan^{-1}\left[\frac{r}{T_c+\frac{D}{2}\cot\phi}\right].$$

At $r=0$, the pressure p of Eq. (9a) shows the maximum value

$$p_{max}=\frac{CV_s}{(T_c+\frac{D}{2}\cot\phi)^2}. \tag{9b}$$

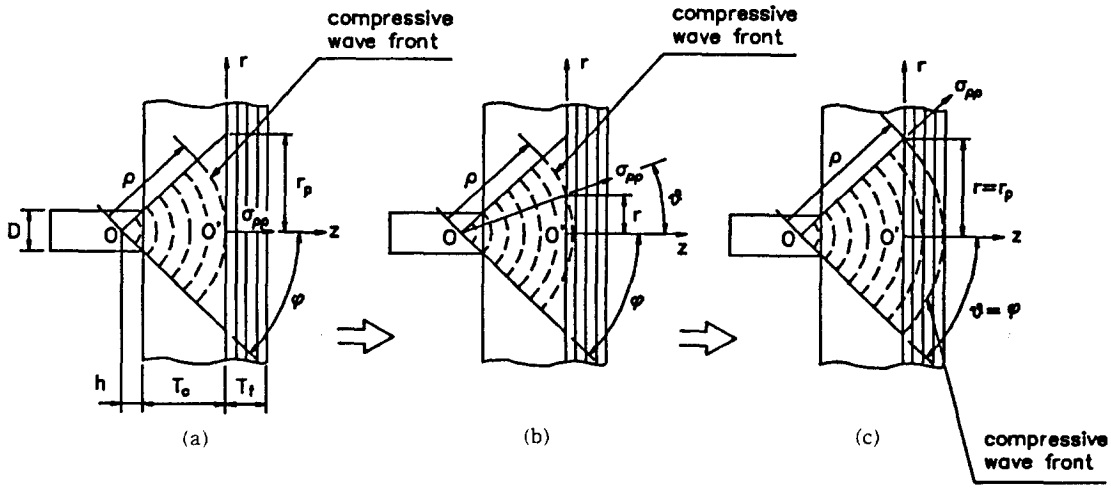

Fig. 3 Schematic diagrams for calculation of the pressure applied on the FRP backing plate.

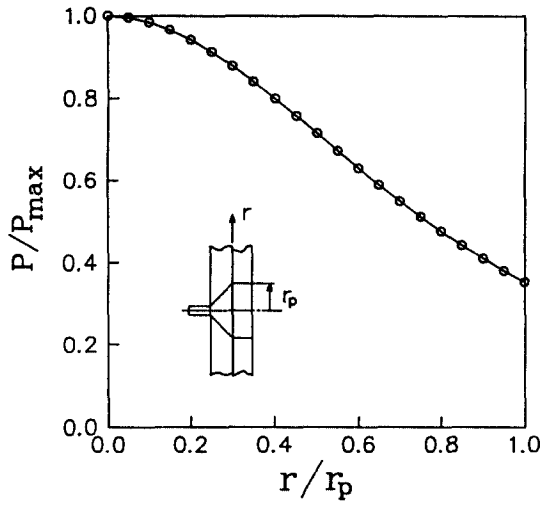

Fig. 4 Distribution of the pressure on the FRP backing plate.

Because the convex surface area of the compressive wave front is proportional to a square of ρ, the pressure reduces with increase of 'r'. Fig. 4 shows the distrbution of the pressure 'p' as a funcition of 'r'.

When an axi-symmetric line load P_1 is applied to a circular plate with clamped boundaries as shown in Fig.5, the z-directional displacement 'w' due to P_1 can be expressed as (Szilard, 1974)

$$w=\frac{P_1}{8D_{pf}}f(r,\ \xi) \tag{10}$$

where for $\xi \leq r$,

$$f(r,\ \xi)=r_p^2 r\left[1-\frac{r^2}{r_p^2}+2\ \ln\frac{r}{r_p}\left[\frac{r^2}{r_p^2}+\frac{\xi^2}{r_p^2}\right]+\frac{\xi^2}{r_p^2}\left[1-\frac{r^2}{r_p^2}\right]\right]$$

and for $\xi \geq r$,

$$f(r,\ \xi)=r_p^2 r\left[1+\frac{r^2}{r_p^2}\left[1+2\ \ln\frac{\xi}{r_p}\right]-\frac{\xi^2}{r_p^2}\left[1+\frac{r^2}{r_p^2}-2\ \ln\frac{\xi}{r_p}\right]\right].$$

since the actual load applied to the backing plate is the pressure given by Eq. (9a), P_1 is related with the pressure 'p' as follows ;

$$P_1=p\ \mathrm{dr}.$$

Since the applied compressive wave load is not only the line load P_1 at $\xi=r$ but also the pressures at $\xi \neq r$ in the whole plate, the Z-directional displacement w_r can be obtained by integrating Eq.(10) as

$$w_r=\frac{1}{8D_{pf}}\left[\int_0^{r_p} f(r^*,\ \xi)\ p(r^*)\ dr^*\right]_{\xi=r} \tag{11}$$

Now, since elastic deformation energy due to P_1 is given by

$$E_{el}=\frac{1}{2}P_1 w_r, \tag{12}$$
$$=\frac{C^2 V_s^2}{8D_{pf}}\int_0^{r_p}\frac{\cos\theta}{[T_c+(D/2)\cot\phi]^2+r^2}\left[\int_0^{r_p}\frac{f(r^*,\ \xi)\cos\theta}{[T_c+(D/2)\cot\phi]^2+r^{*2}}dr^*\right]_{\xi=r}\mathrm{dr}$$

In this model, it is assume that the FRP backing plate is deformed as linear-elastically until the residual projectile strike on the backing plate directly, which passed through the ceramic facing. But after a certain extent of elastic deformation, the FRP begins to rupture. Therefore, on estimating a ballistic limit by this method, it should be examined that the maximum equivalent stress developed in the FRP backing exceeds the tensile strength of the FRP or not before the direct strike.

Since the FRP backing is axi-symmetrically loaded in a circular area (nearly equal to the base of the ceramic fracture conoid) and the maximum pressure is applied at its center as shown in Fig.4, the maximum stress is developed at the rear surface center point of the FRP backing plate. Consequently, at the point of $r=0$ and $z=T_f$,

$$\sigma_{rr}=\sigma_{\theta\theta}=\sigma_{max},\ \text{while others are}\ \sigma_{ij}=0. \tag{13}$$

Also, at the point, σ_{rr} is given by (Szilard, 1974)

$$\sigma_{rr}=\frac{ET_f}{2(1-\nu_f)}\frac{\partial^2 w_r}{\partial r^2} \tag{14}$$

Now, we assume that the FRP would fail according to von-Mises' criterion,

$$\sigma_{eq}=\sqrt{\frac{1}{2}[(\sigma_1-\sigma_2)^2+(\sigma_2-\sigma_3)^2+(\sigma_3-\sigma_1)^2]}\ \geq \sigma_{tf} \tag{15}$$

where σ_{eq} is a equivalent stress and σ_1, σ_2, σ_3 are principal stresses in each direction and σ_{tf} is a tensile strength of the FRP. Substituting Eq. (13) and (14) into Eq. (15), we obtain

$$[\sigma_{eq}]_{max}=[\sigma_{rr}]_{\substack{r=0\\z=T_f}}=\left[\frac{ET_f}{2(1-\nu_f)}\frac{\partial^2 w_r}{\partial r^2}\right]_{\substack{r=0\\z=T_f}}\geq\sigma_{tf} \tag{16}$$

where w_r is given by Eq.(11). The same result can be derived with Tresca's criterion. Using this equation, we can examine that the FRP backing would be ruptured or not when the residual projectile just before striking the FRP backing.

2.4 Penetration of FRP Backing

Generally, the ballistic limit velocity of a uniform metal armor is given by(Zukas, 1981)

$$\frac{Mb_{bl}^2}{D^3}=\alpha\left[\frac{T}{D}\right]^\beta \tag{17}$$

where the constants α, β are dependent on material properties of the projectile and armor, or penetration mechanism. They can be obtained by curve fitting of ballistic test results. Eq. (17) can be rewritten as

$$\frac{MV_{bl}^2}{2}=\frac{\alpha D^3}{2}\left[\frac{T}{D}\right]^\beta. \tag{18}$$

From the definition of the ballistic limit, the kinetic energy of the projectile, the left side terms of Eq(18), will be dissipate during the penetration procedure. It also implies that the energy needed to penetrate a given armor. Consequently, if some ballistic test results can be reduced in Eq.(17), then the constant of α and β can be required from the test result diagram. And then the absorbed energy during penetration though an armor of given thickness T by a projectile of given

diameter D can be simply calculated using Eq.(18). This means that only if material properties of a projectile and an armor are constant, the energy absorbed during penetration of the armor is independent on the length or mass of the projectile but also it is simply given by diameter of the projectile and thickness of the armor.

Even though the length or mass of the residual projectile is reduced during pass through the ceramic facing, the energy E_3 absorbed during penetration of the FRP backing, is equal to the one necessary for penetrating single FRP plate of the same thickness as the backing. With using Eq.(18) the energy is

$$E_3=\frac{\alpha D_3}{2}\left[\frac{T}{D}\right]^{\beta}. \tag{19}$$

Therefore, E_3 can be obtained with substituting α, β (which are obtained for single FRP plates), T_f and D into Eq.(19). Here it should be noticed that Eq.(19) is applicable only in case of the projectile diameter is not changed during penetration of the ceramic facing.

3. RESULTS AND DISCUSSION

In order to prove the validity and to compare the results of this method, Wilkins' experimental and computational results of AD85 ceramic/glass FRP composite armors (Wilkins, 1968) are used. Tables 1 to 3 show the material properties, specifications, and the results.

If striking velocity of a projectile is equal to ballistic limit of an armor, that is, $V_s=V_{bl}$, the residual velocity after penetration V_r is zero. Consequently, Eq.(1) is replaced by

$$\frac{MV_{b1}^2}{2}=E_1+E_2+E_3. \tag{20}$$

E_1, the energy absorbed during penetration of the ceramic facing, can be obtained by substituting Eq. (4) into Eq. (5). Here the constant B in Eq. (4) is taken to be 100 Nm and the angle ϕ in Eq. (5) is taken to be 45 degree from the Fig. 3b in (Wilkins, 1968)

E_2, the energy absorbed during elastic deformation of the FRP backing, is expressed as Eq. (12). But in the equation the ballistic limit V_{bl}, whose value can not be known beforehand, is included. Therefore, instead of E_2, $E_2'=E_2/V_{b1}^2$ is calculated. Here the constant C is taken to be 72.6kg/s by substituting Wilkins' experimental result (Fig.5 in (Wilkins, 1968)) into Eq(9b). (See Appendix A for further particulars on calculation of C.)

E_3, the energy absorbed during penetration of the FRP backing, is given by Eq.(19). Here constants α and β are obtained by reducing experimental results by Du Point Inc. (1980a, 1980b) into Eq.(17). Table 4 shows the cited results and the values of α and β.

Substituting $E_2=E_2'/V_{b1}^2$ into Eq.(20), the ballistic limit V_{b1} is expressed as

$$V_{b1}=\sqrt{\frac{2(E_1+E_3)}{M-2E_2}}. \tag{21}$$

Now, the thing to do for determining the ballistic limit of a given armore is only to substitute E_1, E_2' and E_3 into Eq.(21). At the same time the maximum equivalent stress occurring in

Table 1 Specifications of the projetile and target.

projectile				target	
type	dia. (mm)	mass(g)	material	facing plate	backing plate
sharp nosed AP	7.62	8.12	steel	AD85 ceramic 4.064~ 8.636mm	woven roving glass FRP 3.175~12.7mm

Table 2 Mechanical properties of the AD 85 ceramic.

density ρ	bulk modulus, K	shear modulus, G	compressive strength, σ_{cc}	tensile strength, σ_{tc}
3.43 g/cm³	1.54×10^5 MPa	8.3×10^4 MPa	3.8×10^3 MPa	3.0×10^2 MPa

Table 3 Mechanical properties of the glass FRP backing plate.

density, ρ	Young's modulus, E_f	Poisson's ratio, ν_f	compressive strength, σ_{cf}	tensile strength, σ_{tf}
1.7~1.8 g/cm³	1.7~2.1 ×10 MPa	0.11	2.7×10^2 MPa	3.0×10^2 MPa

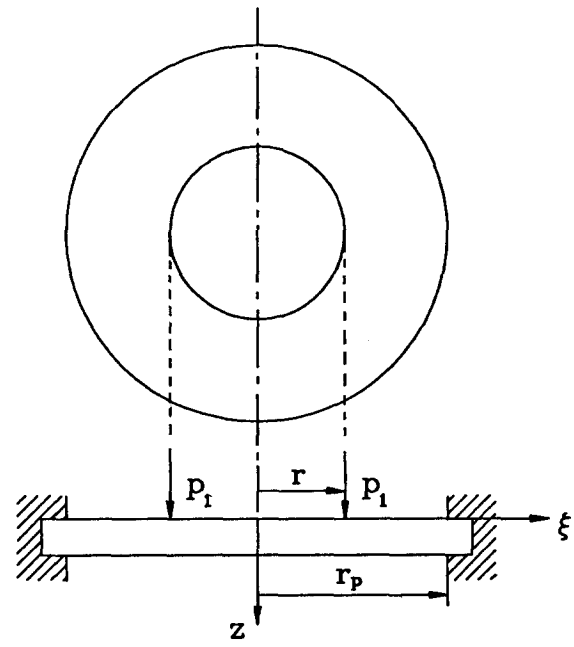

Fig. 5 An axisymmetrically loaded circular plate with clamped edge.

Table 4 Ballistic performances of woven roving glass-FRP plates.[21,22]

No.	area density (kg/m²)	projectile	Projectile mass (g)	ballistic limit (m/s)	α	β
1	6.64	9mm FMJ	8	223	2.186 ×10³ MPa	1.5077
2	10.89	9mm FMJ	8	337		

*FMJ : full metal jacket

the FRP backing should be calculated by Eq. (16) and be checked if the stress does not exceed the tensile strength of the FRP. All calculations are carried out with a simple FORTRAN program.

Table 5 shows the estimated results of ballistic limit in comparison with the ones of experimentally obtained by Wilkins(1968). Here it is found that the estimated results are missing in case of FRP $T_f = 3.175$mm. This fact is believed to be due to an assumption which is builded in this paper as that the FRP backing always behaves elastically during the projectile passing through the ceramic. If the FRP backing is so thin then the backing is severely deformed under the pressure transmitted from the facing, so a local or whole failure may occur in the backing. With this results, it becomes impossible to absorb the elastic deformation energy at the failed region. In this case, with using Eq.(12), E_2' value is over estimated.

Table 5 Wilkins' experimental ballistic limits [7] and calculated ones of AD85/glass-FRP composite armour attacked by 30 cal. AP projectile.

$T_c(mm)$ / $T_f(mm)$	4.064	5.334	6.35	7.874	8.636
3.175	235/	338/	469/	567/	613/
4.445	/338	369/419	500/532	604/816	646/1026
6.35	354/381	491/440	582/515	728/691	850/811
7.62	/434	552/497	671/571	796/736	872/847
9.525	512/526	631/600	735/680	832/847	905/953
12.7	/687	716/789	796/888	899/1072	963/1180

* experimental/calculated
* unit is m/s

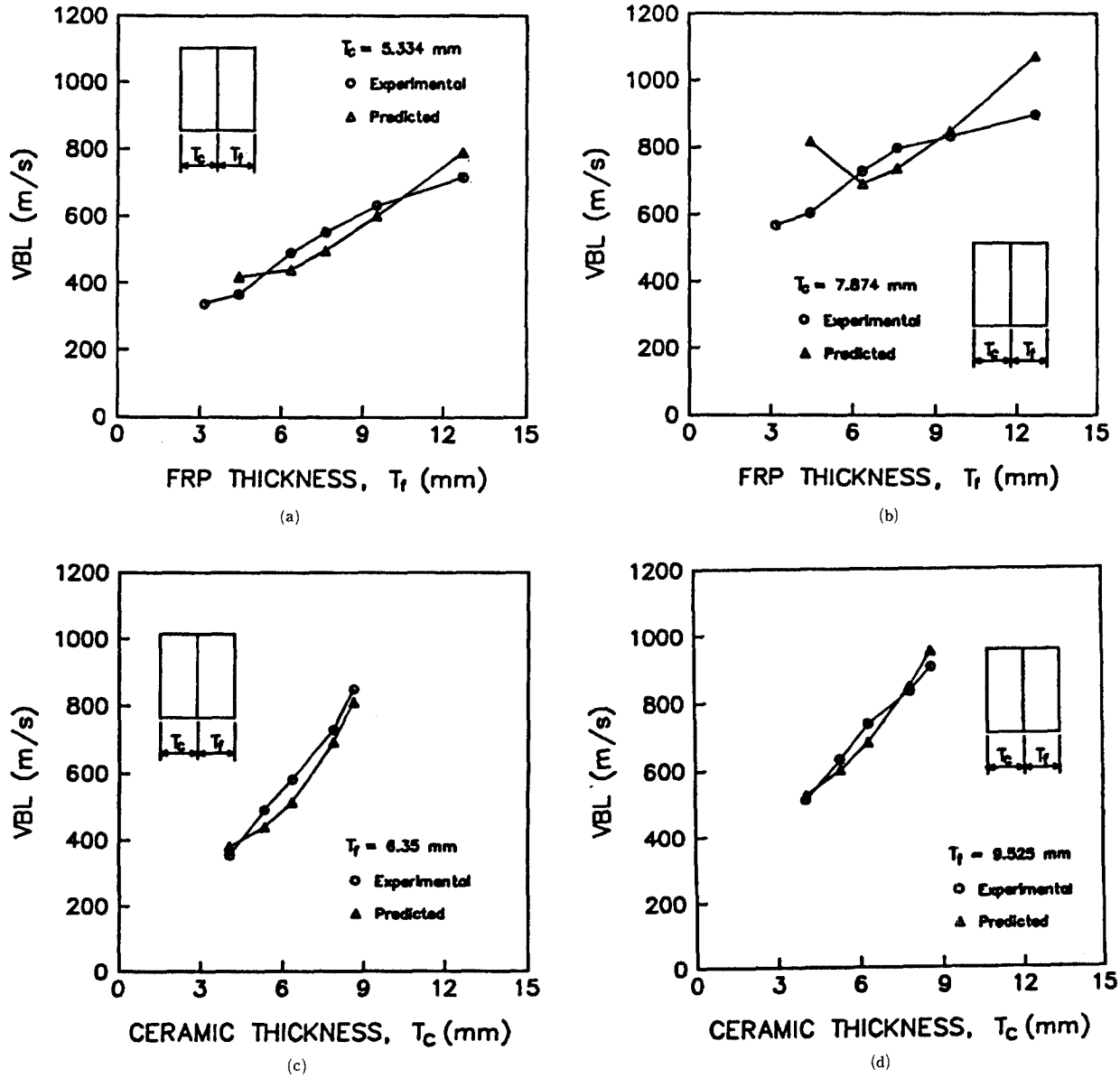

Fig. 6 Experimental results (Wilkins, 1968) and calculated ones for ballistic limit of the AD85/glass-FRP composite armour attacked by a 30 cal. AP projectile.

Consequently, the inner part of $\sqrt{\ }$ in Eq.(21) may become negative and then it becomes impossible to estimate the ballistic limits. On the other while in case of $T_c/T_f=7.874$ mm/4.445mm and 8.636mm/4.445mm, the values of E_2' are also over-estimated, but the inner parts do not become negative. As the result, the maximum equivalent stresses in the FRP by Eq.(16) beocme to be 1022 MPa and 1284 MPa, respectively, which values are much larger than the tensile strength of the FRP. And then the estimated V_{b1}'s show considerable differences from the experimental ones. In case of $T_c/T_f=7.874$mm/12.7mm and 8.636mm/12.7mm, the differences are considerable too. This fact can be explained as follows. Since the stress wave velocity of the FRP are relatively low, but also the ballistic performance of the FRP is limited to the low velocity projectile (Raible, 1980). That is, even though increasing the thickness of the FRP does not guarantee the ballistic resistance enough to shut out a high velocity projectile. Hence Eq.(19), in which constants α and β were evaluated for handguns, is effective only for relatively thin FRP. Therefore, E_3 calculated by use of Eq.(19) may be over-estimated for thick FRP backings (such as $T_f=12.7$ mm), which is believed to be a source of the differences.

Figs. 6(a) and (b) show the estimated and experimental results of ballistic limit as a funcition of the thickness of the FRP backing for the two kinds of the ceramic thickness as $T_c=5.334$mm and 7.874mm. Except for the omitted or over-estimated ones as the above-mentioned reasons, the estimated values of V_{b1} agree well with the experimental ones.

Figs.6(c) and (d) show similar results as a funcition of T_c in case of $T_f=6.35$mm and 7.874mm, respectively. Here the estimated values of V_{b1} fairly well agree with the experimental ones on the whole.

Figs.7(a) to (d) show the energies absorbed during each stage of penetration which are obtained as calculating the

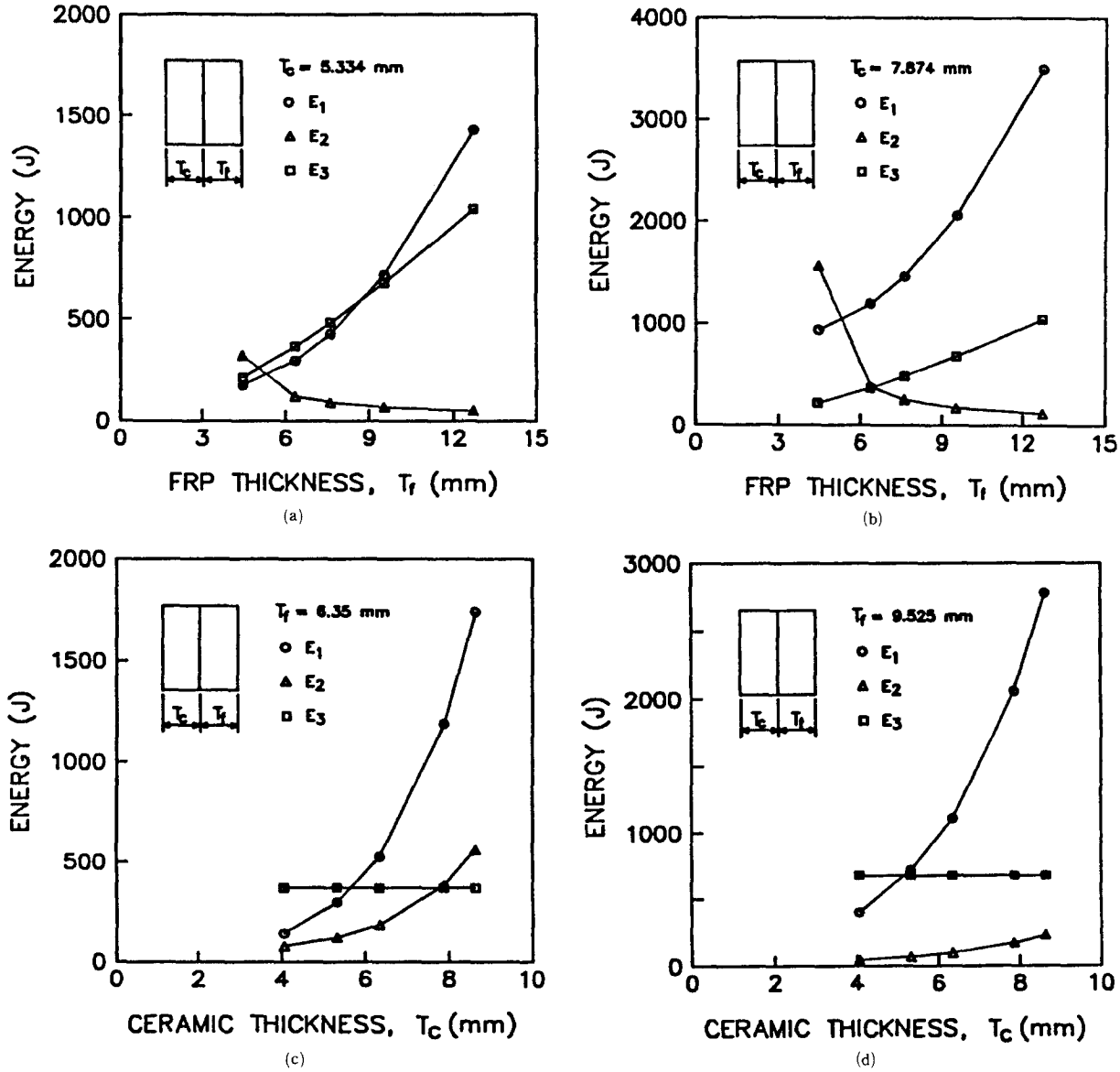

Fig. 7 Calculated energies which are absorbed during penetration of the AD85/glass-FRP composite armour attacked by a cal. 30 AP projectile.

V_{b1}'s shown in Figs.6(a) to (d), respectively.

In case of varying FRP thickness (T_f), while T_c's are kept to be constant as shown in Figs.7(a) and (b), the energies absorbed during penetration of the ceramic facing and the FRP backing, (that is, E_1 and E_3) are rapidly increased as thickening the backing but the energy absorbed during elastic deformation of the backing (E_2) is decreased. The reason can be explained as follows : As thickening the backing, the entire armor is so stiffened that the effective strength of ceramic given by Eq.(4) is increased; Consequently, E_1 by Eq.(5) and E_3 by Eq.(19) are increased too. However the stiffened backing decreases an elastic energy, E_2. In case of the backing is so thick, such as $T_1=12.7$mm, E_3 is as much as 1040 J, which is equivalent to kinetic energy of a cal.30 AP projectile whose velocity is 506m/s. As like this result, E_3 value would be over estimated when the projectile which is just passed through the ceramic facing has still considerable high velocity. This result comes from the Eq.(19), which applicable only for the low velocity region as mentioned earlier. As the result, the estimated V_{b1}'s may show some differences from the experimental ones. On the otherwhile, if the ceramic facing thickness being increased enough, then the mass reduction effect of projectile becomes serious. Especially in the case of the $T_c/T_f=7.874$mm/12.7mm and 8.635 mm/12.7mm, the effective strength of the ceramic is enlarged nearly to its compressive strength according to Eq.(4), so that the mass-reduction of the projectile becomes severe, and also the differences of calculation results become serious as shown in Table 5.

In case of T_c's are changed while T_f's are kept to be constant as Figs.7(c) and (d), thickening the ceramic facing does not only stiffen the entire armor, which increase the effective strength of the ceramic, but also enlarges the volume of the ceramic fracture conoid. Consequently, E_1 is rapidly increased. Simultaneously, the deformation area in the backing (nearly equal to the base area of the fracture conoid) is expanded, so that the E_2 is also increased. E_3, however, is invariable because of the constant thickness of the backing.

The constant B in Eq.(3) and (4) determines how rapidly the effective strength of the ceramic reaches to its compressive strength with increasing of the stiffness-fracture strain product. Although here the constant which is chosen so as to result in a good estimation of V_{b1}, is believed to be a material property of a given ceramic and is needed further investigation.

As shown above, in this paper, the penetration procedure is divided into three stages, and then the energy absorbed in each stage can be quantitatively evaluated. But also appreciate how each of the ceramic and the fRP contributes to the ballistic resistance and influences on each other. Therefore we expect this method to be useful to design optimally a ceramic-FRP composite armor under given circumstances such as specification of an attacking projectile or weight limitation. However, in this method some interface friction or adhesion between the facing and backing is ignored. This fact needs a further study.

4. CONCLUSION

One of a method is proposed to estimate ballistic limits of the ceramic-FRP composite armor using an energy balance approach. As the results of comparison with the experimental data for AD85 ceramic/glass FRP composite armors, it is found that

(1) The ballistic limits of ceramic-FRP can be fairly good estimated with some assumptions in this paper. Such as, the mass reduction ratio of the colliding projectile is not to severe and the penetrating velocity of the projectile through the FRP material is not to high.

(2) The experimental and calculation results are well agreed on the composite armors which consist of 4.064mm to 8.635mm thick AD85 ceramic plate and 4.445mm to 9.925mm thick glass FRP plate.

Someday we can get a free chance for using the power guns, it would be possible to modify the relationship between the fractured conoid shape and the total stiffness of the ceramic materials, mass reduction ratio of each projectile, and also to modify the fracturing phenomena of FRP materials for improving the calculation accuracy and application ranges of our presented study.

APPENDIX A

• calculation of constant C

Eq.(9b) can be replaced by

$$C=\frac{P_{max}\left[T_c+(\frac{D}{2})\cot\phi\right]^2}{V_s}$$

Substituting Wilkins' results and related data (see Figs.3 and 5 in (Wilkins, 1968)) into this equation, the value of C can be calculated. Here, $T_c=0.34''=0.00863$m, $D=0.3''=0.00762$m, $\phi=45°$, and $V_s=2800$ft/sec$=853.44$m/s. And the value of P_{max} is taken at 3.6μsec after a strike, that is, $P_{max}=4$kbar$=4\times10^8$ Pa. The reason is explained as follows : At about 5 μ see after a strike, as shown in Fig. 11 in (Wilkins, 1968), the interface between the ceramic and the backing begins to move backward for the just behind the striking point. This implies that the backing is subject to not only the pressure due to the compressive wave front, but simultaneously the one due to the direct movement of the ceramic. In this method E_2 means the energy due to only the compressive wave while some effect of the direct movement is believed to be comprised in the energy absorbed during penetration of the backing, E_3. Therefore, from Fig.5 in (Wilkins, 1968),we take the P_{max} value at 3.6 μsec after a strike, that is, just before beginning of the movement.

ACKNOWLEDGEMENT

This research was performed under financial support of HANKUK FIBER GLASS CO., LTD. The authors would like to appreciate to Mr. Y.S. Seo, Mr. R.S. Park and Mr. B.G. Choi of ADD(Agency for Defense Developement) for their contributions on this work.

REFERENCES

Bless, S.J., Rozenberg, Z. and Yoon, B., 1987, "Hypervelocity Penetration of Ceramics," Int. J. Impact Engng. Vol. 5, pp. 165~171.

Bodine, E.G., Dunleavy, J.G. and Rolsten, R.F., 1969, "The

Optimization of Composite Ceramic-Armor Materials," Symposium on Ceramic-Armor Technology, Columbus, Ohio.

Cardner, P.B., 1975, "Advances in Ceramic Composite Armor Technology," Symposium on Vulnerability and Survivability, San Diego, California.

Cline, C.F. and Wilkins, M.L., 1969, "The Importance of Material Properties in Ceramic Armor," Symposium on Ceramic-Armor Technology, Columbus, Ohio.

Du Pont De Nemours & Co. Inc, 1980, "Preparation of Composite Armor Reinforced with Fabrics of KEVLAR Aramid."

Du Pont De Nemours & Co. Inc, 1980, "A Guide to Designing and Preparing Ballistic Protection of KEVLAR Aramid."

Evans, A.G., Gulden, M.E., Eggum, G.E. and Rosenblatt, M., 1976, "Impact Damage in Brittle Materials in the Plastic Response Regime." Rockwell International Science Center Report SC 5023-9TR.

Florence, A.L., 1969, "Interaction of Projectiles and Composite Armor-Part II," AMMRC CR69-15, Stanford Research Institute.

Forrestal, M.J., Rosenberg, Z., Luk, V.K. and Bless, S.J., 1987, "Perforation of Aluminum Plates with Conical-Nosed Rods," J. Appl. Mech. Vol.54, pp. 230~232.

Gulbierz, I. and Bohan, C., 1980, "Evaluation of Methods to Increase the Balistic Efficiency of Alumina Face Plates for Alumina/glass-Reinforced Plastic Composite Armor Systems," Picatinny Arsenal Technical Report 3908.

Kim, C.H. and Palmour, H., 1970, "Microstructural Alternations in Alumina Ceramics Associated with Ballistic Impact Events," Technical Report 70-8, North Carolina State University.

Landingham, R.L. and Casey, A.W., 1972, Final Report of the Light Armor Materials Program, UCRL-51269, Livermore, Califonia.

Martin, D.M., 1969, "Pernetration Mechanics," Symposium on Ceramic-Armor Technology, Columbus, Ohio.

Raible, R.C., 1980, "Fibrous Armor," in Ballistic Materials and Penetration Mechanics, edited by Roy C. Laible, Elsevier, pp.73~112.

Rozenberg, Z. and Yeshurun, Y., 1987, "A New Definition of Ballistic Efficiency of Brittle Materials Based on Use of Thick Backing Plates," Conference Impact 87, Bremen, FRG.

Rozenberg, Z. and Yeshurun, Y., 1988, "The Relation between Ballistic Efficiency and Compressive Strength of Ceramic Tiles," Int. J. Impact Engng. Vol.7, pp.357~362.

Stiglich, Jr., J.J., 1968, "A Survey of Potential Ceramic Armour Material," AMMRC MS 68-04, Ceramic Material Research for Army Material.

Szilard, R., 1974, Theory and Analysis of Plates, Prentice-Hall.

Tortil, M.L. and Herrick, J.W., 1971, "Effectiveness of Various Spall Shield Configurations," 73rd Annual Meeting of American Ceramic Society, Chicago, Illinois.

Wilkins, M.L., 1968, Third Progress Report of Light Armor Program, UCRL-50460.

Wilkins, M.L., Cline, C.F. and Honodel, C.A., 1969, Fourth Progress Report of Light Armor Program, UCRL-50694.

Wilkins, M.L., Landingham, R.L., and Honodol, C.A., 1971, Fifth Progress Report of Light Armor Program, UCRL-50980.

Zukas, J.A., 1981, "Penetration and Perforation of Solids," in Impact Dynamics, edited by Jonas A. Zukas et al, John Wiley & Sons, pp.152~214.